

Supporting Information

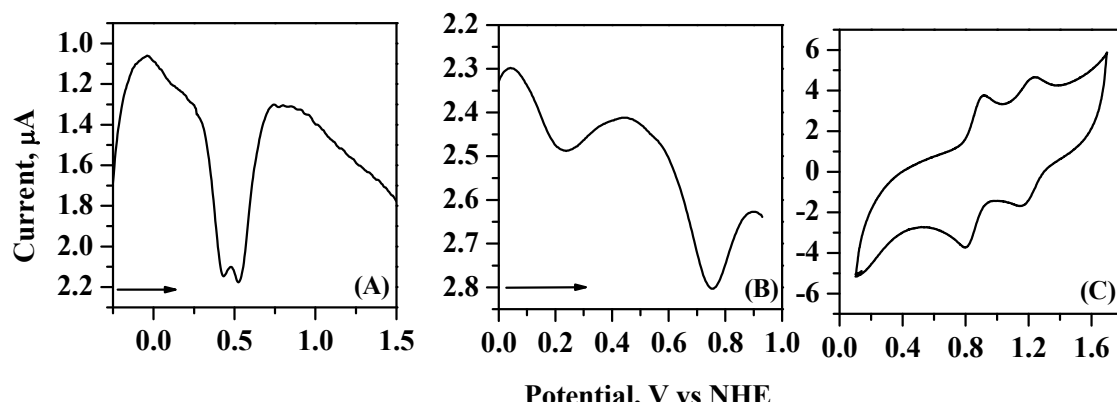


Figure S1 – Differential Pulse Voltammetries at 0.02 V/s of (A) $\{[\text{Ru}^{\text{II}}(\text{NH}_3)_4(\text{pyS})]_2\text{-}\mu\text{-pySSpy}\}^{4+}$ and (B) $\{[\text{Ru}^{\text{II}}(\text{NH}_3)_4(\text{pyS})]_2\text{-}\mu\text{-pz}\}^{4+}$; (C) Cyclic voltammogram at 0.1 V/s of $\{[\text{Ru}^{\text{II}}(\text{NH}_3)_4(\text{pyS})]_2\text{-}\mu\text{-DCB}\}^{4+}$. Glassy carbon and platinum as working and auxiliary electrodes, respectively, in CH_3COONa ($\text{pH} = 3.0$).

Table S1 – Spectroscopic data for MLCT transitions of $\{[\text{Ru}^{\text{II}}(\text{NH}_3)_4(\text{pyS})]_2\text{-}\mu\text{-L}\}^{4+}$ type complexes in different solvents.

L	λ , nm					Tentative assignments	
	$(\epsilon \times 10^{-3}, \text{Lmol}^{-1}\text{cm}^{-1})$						
	Water	Acetonitrile	Acetone	DMSO	DMF		
DTDP	461(68)	472(17)	474(12)	497	504(9.4)	$\pi^*(\text{pyS}) \leftarrow \text{d}\pi(\text{Ru}^{\text{II}})$	
	590(1.2)	609(0.8)	600(0.6)	620	675(2.4)	$\pi^*(\text{pySSpy}) \leftarrow \text{d}\pi(\text{Ru}^{\text{II}})$	
pz	485(1.8)	477(5.6)	487(2.6)	419	416	$\pi^*(\text{pyS}) \leftarrow \text{d}\pi(\text{Ru}^{\text{II}})$	
	587(1.0)	589(3.3)	610(0.9)	518	512	$\pi^*(\text{pz}) \leftarrow \text{d}\pi(\text{Ru}^{\text{II}})$	
DCB	456(62)	457(22)	440(12)	504(25)	496(20)	$\pi^*(\text{pyS}) \leftarrow \text{d}\pi(\text{Ru}^{\text{II}})$	
	-	613(0.2)	-	-	-	$\pi^*(\text{DCB}) \leftarrow \text{d}\pi(\text{Ru}^{\text{II}})$	

Table S2 – Relative intensities of selected resonance Raman bands of $\{[(\text{pyS})\text{Ru}(\text{NH}_3)_4]_2\text{-}\mu\text{-L}\}(\text{PF}_6)_4$ type complexes excited by different wavelengths (λ_0).

Relative intensities				
L	ν^*/cm^{-1}	λ_0/nm	Assignment ^{27,33-42}	
		647.1 568.2 488.0		
	289	0.44 0.39 0.00		skeletal

	383	0.20	0.13	0.00	skeletal
pySSpy	415	0.51	0.48	0.00	$\delta(\text{CCC}) + \nu(\text{CS})$ pySSpy
	515	0.42	0.29	0.06	$\nu(\text{SS})$ pySSpy
	698	0.67	0.49	0.13	$\delta(\text{CCC}) + \nu(\text{CS})$ pySSpy
	1021	0.69	0.93	0.72	1a ring breathing pySSpy + pyS
	1057	0.42	0.41	0.44	ring breathing ring breathing
	1119	0.35	0.44	0.48	12a ₁ ring breathing + $\nu(\text{C=S})$ pyS
	1219	0.63	0.99	1.32	$\beta(\text{CH})$ pyS
	1289	0.43	0.37	0.18	$\beta(\text{CH})$ pySSpy
	1461	0.40	0.40	0.14	$\nu(\text{CC})$ pySSpy + pyS
	1500	0.27	0.32	0.15	$\nu(\text{CC})$ pySSpy + pyS
	1595	0.94	1.61	1.58	$\nu(\text{CC})$ pyS
pz	300	0.34	0.33	0.14	skeletal
	390	0.29	0.00	0.00	$\nu(\text{RuN})$ pz
	1024	0.72	0.74	0.52	1a ring breathing pz + pyS
	1056	0.21	0.22	0.18	$\beta(\text{CH})$ pz + pyS
	1076	0.16	0.31	0.44	12a ₁ ring breathing pyS + v(C=S)pyS
	1230	1.22	1.79	1.48	$\beta(\text{CH})$ pz + pyS
	1599	1.37	2.01	1.92	$\nu(\text{CC})$ pz + pyS
DCB	289	0.09	0.07	0.01	skeletal
	413	0.12	0.07	0.01	skeletal
	1023	0.14	0.15	0.10	1a ring breathing DCB + pyS
	1123	0.07	0.09	0.07	12a ₁ ring breathing + $\nu(\text{C=S})$ pyS
	1179	0.20	0.25	0.36	$\beta(\text{CH})$ DCB
	1220	0.19	0.19	0.17	$\beta(\text{CH})$ DCB + pyS
	1600	0.42	0.61	0.64	$\nu(\text{CC})$ DCB + pyS
	2223	0.07	0.11	0.11	$\nu(\text{C}\equiv\text{N})$ DCB

*Wavenumbers related to spectra at 647.1 nm.

The spectroelectrochemical measurements were carried out in a thin layer cell with gold grid, gold wire and Ag/AgCl (BAS, 3.5 M KCl) as working, auxiliary and reference electrodes, respectively. An aqueous solution containing 0.1 mol L^{-1} CH_3COONa ($\text{pH} = 3.0$) was used as electrolyte medium. The spectra were acquired according to the electrochemical data of the compounds. Accordingly, at first, it was applied a potential to oxidize one metal center ($E_{\text{apl}} = E'(1)$) followed by the respective reduction ($E_{\text{apl}} < E'(1)$) and second it was applied a potential to oxidize both metal centers ($E_{\text{apl}} = E'(2)$) followed by the reduction of both ($E_{\text{apl}} < E'(2)$). For $\{\text{[Ru}^{\text{II}}(\text{NH}_3)_4(\text{pyS})\}_2\text{-}\mu\text{-DCB}\}^{4+}$, the spectra were first acquired with an applied potential of 0.6 vs Ag/AgCl. As can be seen in the spectra illustrated in Figure S3, the intensity of the band at 445 nm, which is assigned to the MLCT transition from Ru^{II} to pyS ligand (this transition is observed at 456 nm in water without electrolyte), decreases with time at $E_{\text{apl}} = 0.6 \text{ V}$ vs Ag/AgCl. The reversibility of the process is evidenced by the recovery of the band at 445 nm when $E_{\text{apl}} = 0.1 \text{ V}$ Ag/AgCl which is sufficient to reduce both the metal centers. The insets show the profile of current in function of time during the electrolysis.

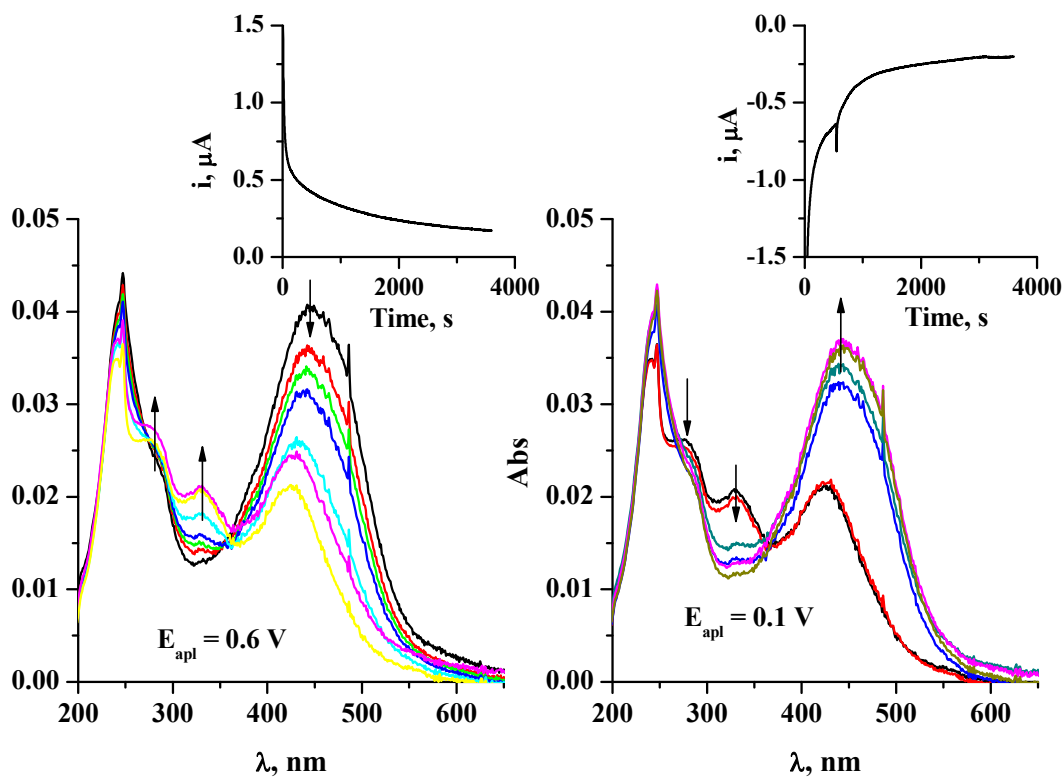


Figure S2 – Absorption spectra obtained during controlled potential electrolysis in 0.1 mol L^{-1} CH_3COONa ($\text{pH} = 3.0$) containing $\{\text{[Ru}^{\text{II}}(\text{NH}_3)_4(\text{pyS})\}_2\text{-}\mu\text{-DCB}\}^{4+}$. Insets: i vs time during electrolysis.

For one-electron oxidation, similar profiles are observed for all the synthesized complexes. However, for $\{\text{[Ru}^{\text{II}}(\text{NH}_3)_4(\text{pyS})\}_2\text{-}\mu\text{-pySSpy}\}^{4+}$ the reversibility is not observed after two-

electron oxidation. Figure S3 shows the spectra acquired at different stoichiometric ratio of $\text{K}_2\text{S}_2\text{O}_8$.

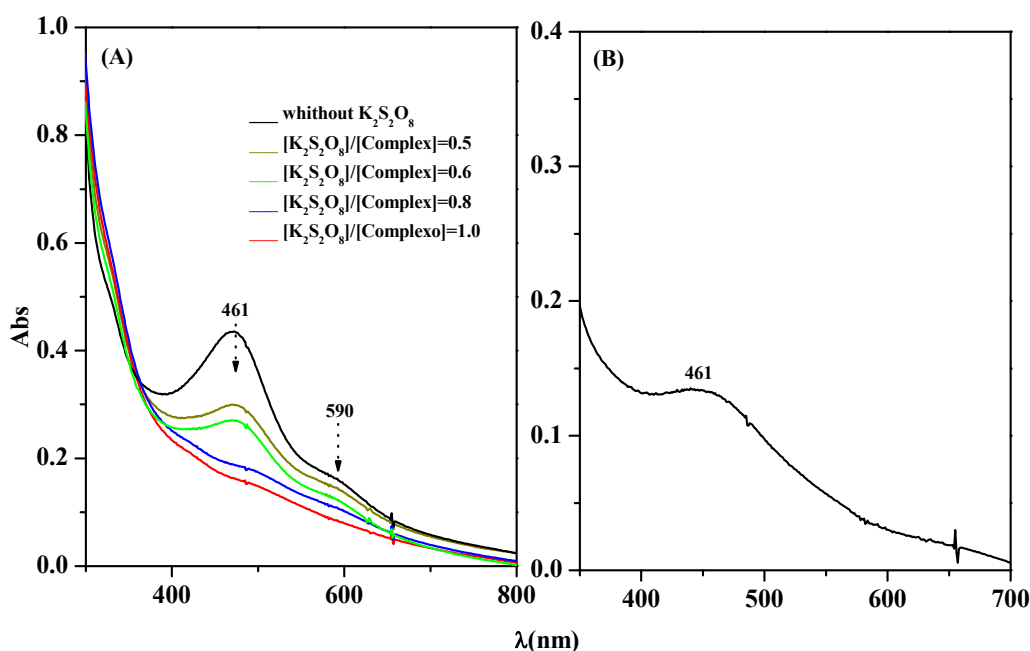


Figure S3 – Absorption spectra obtained (A) after the addition of different ratio of $\text{K}_2\text{S}_2\text{O}_8$ and (B) after the addition of zinc amalgam.

According to the spectra above, the intensity of the bands assigned to the MLCT transition of Ru^{II} to pyS and pySSpy ligands at 461 and 590 nm, respectively, decreases as the oxidant agent is added. After complete oxidation of the two metal centers ($\text{K}_2\text{S}_2\text{O}_8/\text{Complex} = 1.0$), zinc amalgam was aged to the solution in order to reduce the metal centers and recover the spectrum profile of the fully reduced binuclear compound. However, as can be seen in Figure S3 (B), the band at 590 nm is no longer observed. Although, without experimental evidence, we guess that this result can be assigned to the reduction of SS bonding of pySSpy resulting in the formation of two monomers as suggested in the scheme below:

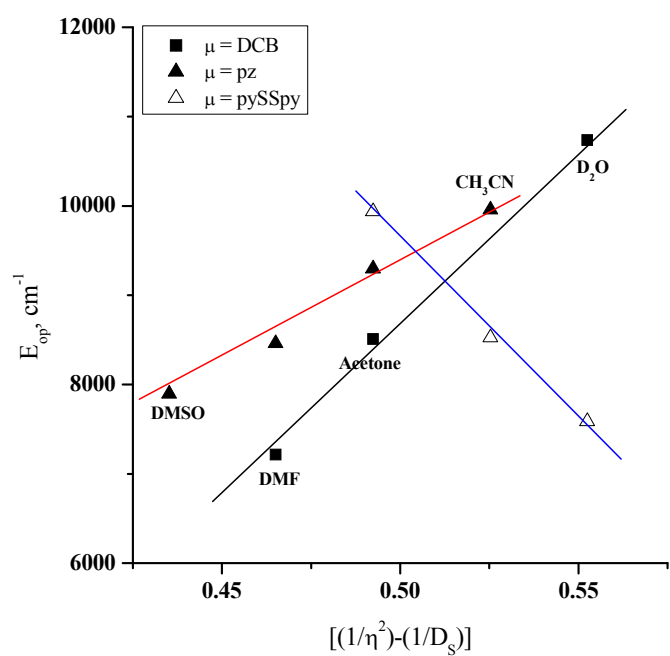
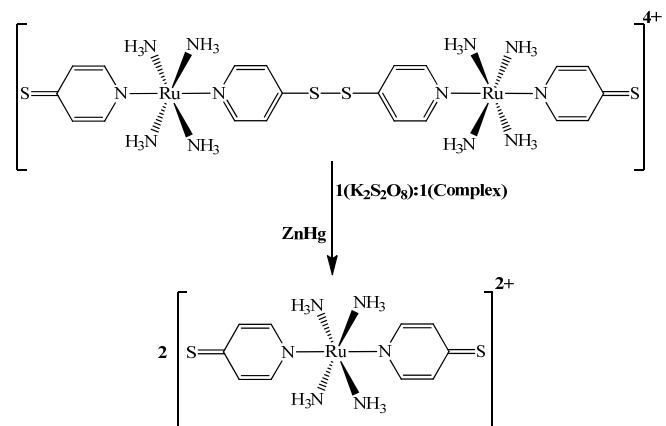


Figure S4 – Plots of E_{op} vs $[(1/\eta^2) - (1/D_s)]$ at different solvents.